ISSN 2070-2051, Protection of Metals and Physical Chemistry of Surfaces, 2010, Vol. 46, No. 6, pp. 727–733. © Pleiades Publishing, Ltd., 2010.

PHYSICOCHEMICAL PROBLEMS OF MATERIALS PROTECTION

The Inhibition Effect of Amides on Aluminium Corrosion in Chloride Solutions[1]

S. Zor and H. Özkazanç

Department of Chemistry, Kocaeli University, 41380, Umuttepe Kocaeli, Turkey

e-mail: merve@kou.edu.tr, szor2001@yahoo.com

Received October 28, 2009

Abstract—The inhibition effect of different concentrations of benzamide (BA), sulfanilamide (SA), and thioacetamide (TA) on the corrosion of aluminium in 0.1 M NaCl solution was investigated by the methods of potentiodynamic polarization, electrochemical impedance spectroscopy, and SEM (scanning electron microscope) in this study. Impedance measurements showed that the charge transfer resistance increased whereas double layer capacitance decreased with the increase in the inhibitor concentrations. Adsorption of these inhibitors followed the Langmuir adsorption isotherm. Thermodynamic parameters of adsorption (K_{ads}, ΔG_{ads}) of studied amides were calculated by using Langmiur adsorption isotherm. The surface films of the aluminium, both in solutions with and without the inhibitors, were then investigated by SEM. The results obtained showed that thioacetamide was much more effective in aluminium inhibition.

DOI: 10.1134/S2070205110060171

1. INTRODUCTION

Aluminium is an important material for use in many industrial applications, such as production of automobiles, radiators, aviation, household appliances, pipes, air conditioners, and electronic devices due to its relatively low cost, high electrical and thermal conductivities, low density, and high corrosion resistance [1–3]. The corrosion resistance of aluminium arises from its ability to form a natural oxide film on its surface in wide variety of media [4–10]. Consequently, the corrosion mechanism of aluminium in chloride solutions has been investigated in a number of studies [11–14] as a popular research subject.

Among many methods of corrosion control and prevention, the use of organic inhibitors is the most frequently used one. Organic inhibitors are mostly used to protect aluminium and alloys against corrosion in aggressive electrolytes because they adsorb on the surface by acting as a protective film on anodic and cathodic areas simultaneously [12, 15]. Most of organic compounds contain polar groups such as nitrogen, sulfur, and oxygen [1–10]. The inhibition of organic compounds is based on the adsorption ability of their molecules. The inhibitor molecules are bonded on the metal surface as chemisorptions, by physical adsorption, or by complexation with the polar groups acting as the reactive centers in the molecules [9].

Adsorption characteristics of these inhibitors depend on a few factors; such as the surface charge of the metal, the chemical structure of organic inhibitors, the distribution of charge in the molecule, the type of aggressive electrolyte, and the type of interaction between the organic molecules and the metallic surface [9, 10, 12, 16, 17].

Amides are organic molecules that contain atoms with high electron levels, such as N, O, and S, in their molecular structures. Some amides and derivatives e.g. urea (U), thiourea (TU), thioacetamide (TA), and thiosemicarbazide (TSC) have been found to be good inhibitors for mild steel in acid solutions [18, 19]. Relationship between molecular structures of these amides and their inhibition efficiencies have been studied in several research reports [18–21]. The inhibition efficiencies of amides on steel have been generally studied in the literature whereas their effects on aluminium have not been studied much. Therefore, the effects of benzamide (BA), sulfanilamide (SA), and thioacetamide (TA) in 0.1 M NaCl on aluminium corrosion were investigated by electrochemical methods (potentiodynamic polarization and impedance spectroscopy). Moreover, their suitable adsorption isotherms were determined by the examination of their adsorption characteristics. The change in the surface structure of aluminium, both in the solutions with and without inhibitors, was determined with SEM.

2. EXPERIMENTAL

All chemicals were of analytical reagent grade (Merck). An aqueous solution of 0.1 M NaCl was used as a blank solution. Amides (Benzamide (BA), sulfanilamide (SA), and thioacetamide (TA)), which were obtained commercially, was added to the chloride solution ranging from 25ppm to 100 ppm. The molecular structures of the studied inhibitors are shown in

[1] The article is published in the original.

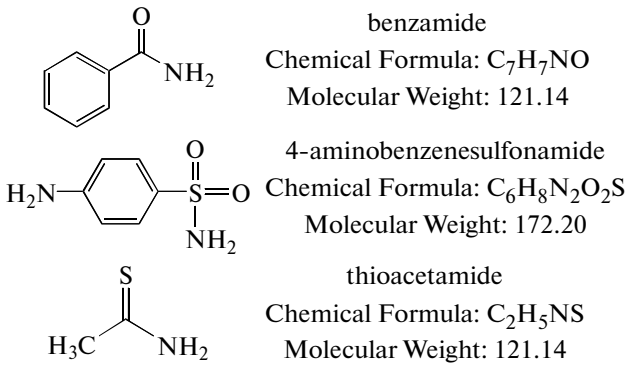

Fig. 1. Structure of inhibitor molecules.

Fig. 1. All experiments were carried out at room temperature with the electrolyte solution in equilibrium with the atmosphere (aerated solutions).

Electrochemical measurements were performed in a classical three electrodes assembly method; with aluminium as the working electrode, a platinum wire as the counter electrode, and a saturated calomel electrode (SCE) provided with a luggin capillary as the reference electrode. The commercially obtained Al was used in all experiments. A cylindrical aluminium rod, whose exposed surface is 0.785 cm^2, was inserted in a Teflon tube so that only the flat surface was in contact with solution.

Prior the electrochemical measurements, the WE was abraded with emery papers (grade 320-400-800-1200), washed with distilled water and methanol, dried at room temperature, and finally immersed to cell. After the immersion of the specimen, a stabilization period of 60 min. was needed to attain a stable value that proves it to be sufficient for open circuit potential. The potentiodynamic polarization curves were obtained from −250 mV versus OCP to +250 mV versus OCP with a scan rate of 5 mV/s. Electrochemical parameters (I_{corr}, E_{corr}, R_p, Corr Rate (mpy)) were obtained from polarization curves.

Impedance measurements were performed at the open circuit potential. Computer controlled EIS measurements carried out on steady state open circuit potential (OCP) disturbed with amplitude of 5 mV a.c Sine Wave, at frequencies between 10^5 Hz–0. 1 Hz, were realized for impedance measurements. Electrochemical measurements, on the other hand, were carried out with a Gamry Instrument Potentiostat/Galvonastate/Reference 600. Echem Analyst Software was finally used for plotting, graphing, and fitting data.

2.1. SEM Analysis

SEM photographs obtained from aluminium surface after specimen immersion in two sets of 0.1 M NaCl solutions, with and without 100 ppm of BA, SA, and TA, for 5 days.

3. RESULTS AND DISCUSSIONS

3.1. Potentiodynamic Polarization Measurements

Polarization curves of aluminium in 0.1 M NaCl solutions, both containing and not containing BA, SA, and TA at various concentrations, was given in Figures 2, 3, and 4 respectively. Anodic and cathodic current densities of all inhibitors decreased as can be seen from the figures. The decrease in cathodic cur-

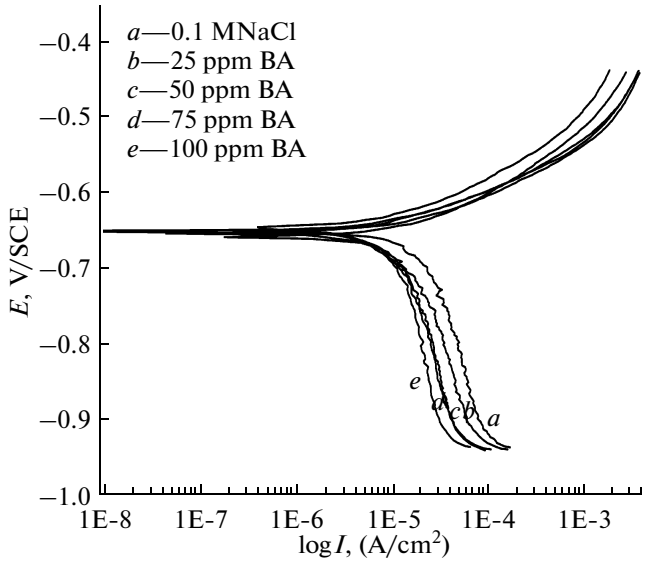

Fig. 2. Polarization curves of aluminium in 0.1 M NaCl in the absence and presence of benzamide.

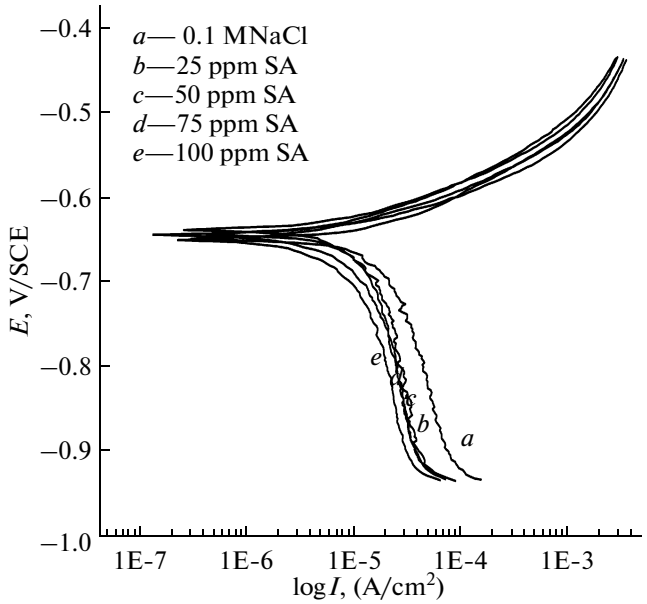

Fig. 3. Polarization curves of aluminium in 0.1 M NaCl in the absence and presence of sulfanilamide.

rent densities was observed to be more. Accordingly, for the inhibition effects of the molecules, though they seem as mixed inhibitors, cathodic effect is more dominant as depicted in tafel curves (Figs. 2–4). The decrease in the cathodic current density in TA is especially high (Fig. 4). This decrease was observed more also when the concentration of inhibitors was increased. The blockage of metal surface by inhibitors decreased the cathodic reduction rate (Figs. 2–4).

Electrochemical parameters such as corrosion potential (E_{corr}), corrosion current density I_{corr}), polarization resistance (R_p), and corresponding inhibition efficiency (IE) values for different inhibitor concentrations are given Table 1. The inhibition efficiencies at different inhibitor concentrations were calculated from the Eq. (1);

$$\mathrm{IE}\% = \left[\frac{(i_{corr})_o - (i_{corr})_{inh}}{(i_{corr})_o}\right] \times 100, \qquad (1)$$

where $(i_{corr})_o$ and $(i_{corr})_{inh}$ are the corrosion current densities without and with addition of inhibitor.

Corrosion current densities decreased as the inhibitor concentrations increased as can be seen from Table 1. The decrease in corrosion current density of TA was more than the decreases in BA and SA (Table 1). Polarization resistance and corrosion current density are inversely proportional. The lowest value of corrosion current density (100 ppm TA I_{corr} = 0.25 μA cm^{-2}) corresponded to the highest value of polarization resistance (100 ppm TA R_p = 33650 Ω). The corrosion potential for benzamide and sulfanilamide did not change in significant amounts compared to the 0.1 M NaCl . The corrosion potential for thioacetamide, since the decrease in cathodic current density was more, shifted to more negative values (from −0.653 V to −0.721 V). Inhibition efficiency increased as the inhibitor concentration increased. This increase was the highest in 100 ppm thioacetamide with a percentage of 98.1% (Table 1).

Inhibition efficiency was calculated by polarization resistance with the equation below;

$$\mathrm{IE}\% = \left[\frac{(R_p)_{inh} - (R_p)_o}{(R_p)_{inh}}\right] \times 100, \qquad (2)$$

where $(R_p)_{inh}$ and $(R_p)_o$ are the polarization resistances of solutions with and without inhibitors, respectively.

Inhibition efficiency, which is determined according to the polarization resistance, and inhibition efficiency, which is determined according to the corrosion current density, has similar values in Table 1.

The inhibition efficiencies (IE%) of these compounds followed the sequence TA > SA > BA; this behavior can be attributed to the presence of electron donating groups (sulfur, nitrogen) in the compound TA. The presence of free electron pairs in sulfur and nitrogen atoms favors the adsorption of compound TA on Al surface [17].

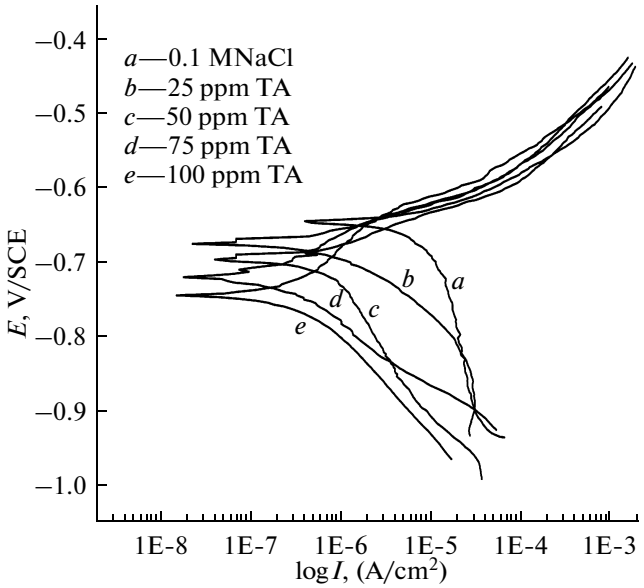

Fig. 4. Polarization curves of aluminium in 0.1 M NaCl in the absence and presence of thioacetamide.

3.2. Impedance Spectroscopy

Figures 5–7 show the Nyquist plots for aluminium in electrolyte solutions with or without the containment of different concentrations of BA, SA and TA. It is clear that the impedance response of aluminium had significantly changed after the addition of amides in the corrosive solutions. This result indicates that the

Table 1. Electrochemical polarization parameters for aluminium electrode in 0.1 M NaCl without and with different concentrations of BA, SA and TA

C, ppml	I_{corr} (μA cm^{-2})	% IE (from I_{corr})	$-E_{corr}$ (V)	R_p (Ω cm^2)	% IE (from R_p)	Corr Rate (mpy)
NaCl	13.12		0.653	1042		17.28
25 BA	12.52	4.57	0.650	1103	5.5	17.06
50 BA	11.34	13.6	0.650	1217	14.4	16.46
75 BA	9.96	24.1	0.646	1381	24.5	15.85
100 BA	8.89	32.2	0.653	1545	32.5	14.93
25 SA	11.15	15	0.640	1235	15.6	16.38
50 SA	8.92	32	0.645	1446	27.9	15.12
75 SA	7.95	39.4	0.646	1602	34.9	13.73
100 SA	5.88	55.2	0.651	2179	52.2	9.30
25 TA	1.02	92.2	0.696	9180	88.6	0.98
50 TA	0.91	93	0.673	12490	91.6	0.74
75 TA	0.51	96.1	0.682	20110	94.8	0.52
100 TA	0.25	98.1	0.721	33650	96.9	0.38

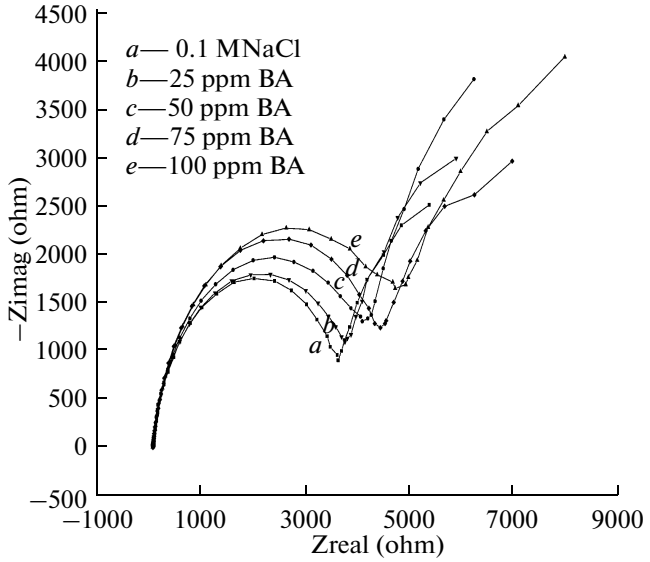

Fig. 5. Nyquist plots of aluminium in 0.1 M NaCl in the absence and presence of benzamide.

impedance behavior increases with increasing concentrations of amides. Characteristic features of the figures related to BA and SA are the presences of a diffusive contribution at low frequencies that is called Warburg Impedance (Figs. 5–6). This indicates that the dissolution mechanism of aluminium is controlled by the mass transport rate both in the absence and presence of the inhibitors [21] The Warburg impedance could be attributed to the oxygen transport from the bulk solution to the aluminium surface. Nyquist plots of Al in 0.1 M NaCl solution with different concentrations of TA is shown in Fig. 7. The Warburg impedance was not observed at Nyquist diagrams related to TA. Thus, the curves are depressed in nature in the figure. This observation was due to the origin of microroughress and other inhomogenities of the solid electrode/solution interface formed during corrosion [12]. The curves also show a single semicircle indicating the occurrence of a single charge transfer reaction (Fig. 7). The analysis of all the impedance plots in terms of the equivalent circuit could be seen in Fig. 8. R_s is the solution resistance, R_{ct} is the charge transfer resistance, Z_w is the Warburg impedance, and CPE is the constant phase element whose impedance is given by [22].

$$Z(\mathrm{CPE}) = 1/T(J_\omega)^n, \tag{3}$$

where J is the imaginary unit, ω is the angular frequency, T is the double -layer capacitance quantity; and n represents the fractional exponent, for which the solid electrode/solution interfaces usually assume the values; $1 > n > -1$ [22]. Considering that the impedance of a double layer does not behave as an ideal capacitor, CPE is most often used to describe the frequency dependence of non ideal capacitive behavior [23]. CPE was substituted for the respective capacitor of C_{dl} in order to fit better the depressed semicircles [12, 22]:

$$C_{dl} = Y_o(\omega''_m)^{n-1}, \tag{4}$$

where C_{dl} is the double layer capacitance, Y_o is the CPE constant, ω''_m is the angular frequency at which imaginary impedance (Z") is maximum, and n is the CPE exponent. The charge transfer resistance was obtained from the diameter value of the semicircle in

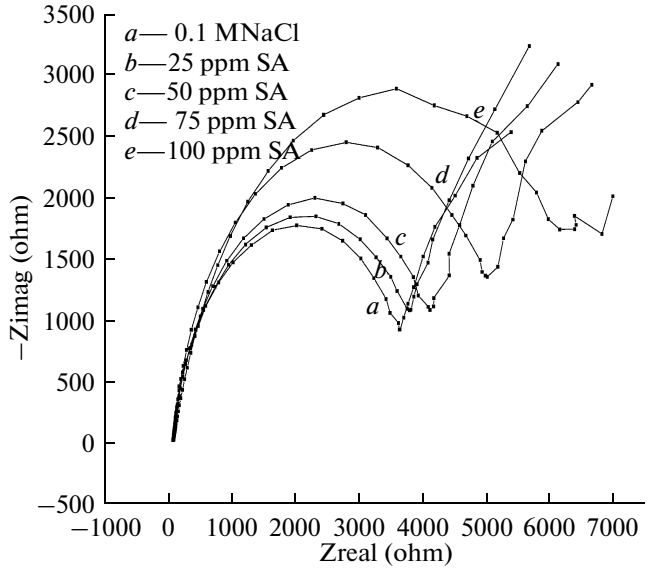

Fig. 6. Nyquist plots of aluminium in 0.1 M NaCl in the absence and presence of sulfanilamide.

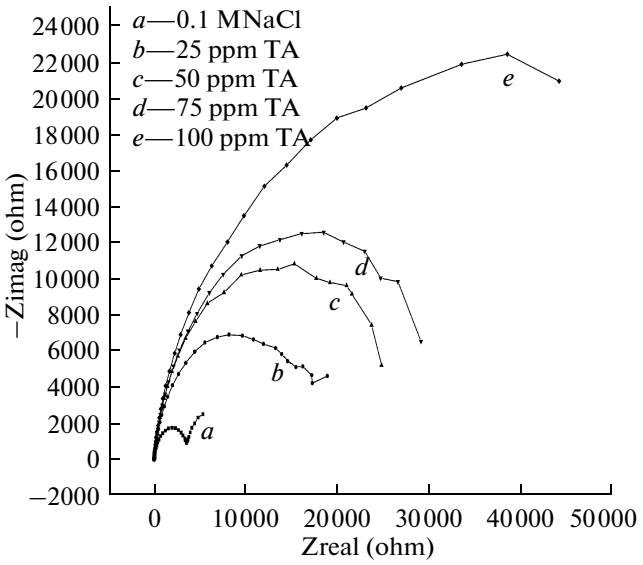

Fig. 7. Nyquist plots of aluminium in 0.1 M NaCl in the absence and presence of thioacetamide.

Table 2. Electrochemical impedance parameters for a aluminium electrode in 0.1 M NaCl without and with different concentrations of BA, SA and TA

C (ppm)	R_s (Ω cm^2)	R_{ct} (Ω cm^2)	$Y_0 \times 10^{-6}$ (Ω^{-1} cm^{-2})	C_{dl} (μF cm^{-2})	n	IE % (R_{ct})
NaCl	49.28	3241	10.67	9.5	0.92	–
25 BA	42.67	3471	10.40	9.2	0.917	5
50 BA	43.98	3684	10.15	9.05	0.918	11
75 BA	50.02	4174	9.86	8.8	0.923	23
100 BA	46.86	4387	9.31	8.3	0.907	26
25 SA	41.57	3650	9.34	8.42	0.931	11
50 SA	49.16	4331	9.08	8.2	0.92	25
75 SA	45.10	4683	8.95	8.0	0.918	31
100 SA	52.42	6601	7.81	6.47	0.84	51
25 TA	42.36	19540	7.76	7.4	0.828	83
50 TA	48.87	24400	6.18	6.5	0.896	87
75 TA	47.0	32360	5.1	5.4	0.891	90
100 TA	47.7	45690	3.25	3.6	0.887	94

Nyquist representation. Inhibition efficiency of the inhibitor was calculated by Eq. (5):

$$IE\% = \frac{(R_{ct})_n - (R_{ct})_o}{(R_{ct})_{inh}}, \quad (5)$$

where $(R_{ct})_{inh}$ and $(R_{ct})_0$ are the values of the charge transfer resistance observed in the solutions with and without inhibitors, respectively. The inhibition efficiencies showed a similar trend with those obtained from the potentiodynamic polarization curves (see Table 1).

The impedance parameters such as R R_{ct}, Y_0, and n obtained from the curves in Figs. 5–7 could be seen in Table 2. Table 2 shows that the R_{ct} values increased with the increase in the inhibitor concentration. The higher R_{ct}, the lower the aluminium corrosion rate and more efficient is the inhibitor. It can be suggested that a protective layer covers the surface of the electrode. The C_{dl} values tend to decrease while R_{ct} and inhibition efficiency values increase. The decrease in the C_{dl} is the due to the decrease in local dielectric constant and/or an increase in the thickness of the electrical double layer. This result indicates that the inhibitor adsorbs at the metal-solution interface [12, 24]. According to the obtained impedance parameters, it can be understood that TA is more efficient for the prevention of aluminium corrosion in 0.1 M NaCl than BA and SA since its R_{ct} values are higher and C_{dl} values are lower.

The protection capacities of BA and SA are not high enough to act as inhibitors. The best inhibition efficiency was also obtained for TA at 100 ppm concentration level. The data obtained from EIS are in good agreement with that from potentiodynamic polarization.

3.3. Adsorption Isotherms

Adsorption behavior provides information about the interactions among the adsorbed molecules as well as their interactions with the electrode surface [12, 16, 22]. The adsorption of organic molecules in metal interface changes according to the molecules' chemical structure, composition of the solution, and electrochemical potential in the metal/solution interface [12, 16]. Adsorption isotherms are often shown to demonstrate the performance of organic adsorbent type inhibitors. Langmuir adsorption isotherm was found to be the best description of the adsorption behavior of the studied inhibitors among several adsorption isotherms described by the following equations.

$$\ln(\theta/\theta - 1) = \ln K + \ln C_{inh}, \quad (6)$$

$$K = \frac{1}{55.5}\exp(-\Delta G_{ads}/RT). \quad (7)$$

C_{inh} is the molar inhibitor concentration in the bulk solution, 9 is the degree of surface coverage $\left[\theta = \left(\frac{IE\%}{100}\right)\right]$, K is the equilibrium constant of the process of adsorption or adsorption coefficient, and ΔG_{ads} is the standard free energy of adsorption. Figure 9

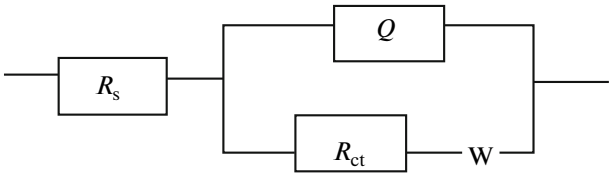

Fig. 8. Equivalent circuit model for impedance curves.

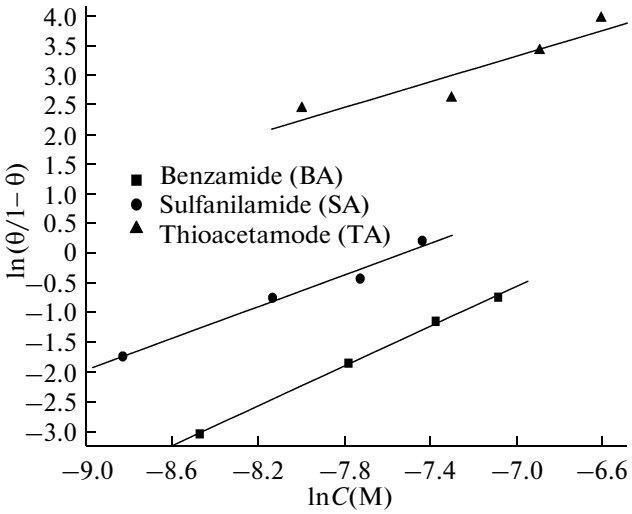

Fig. 9. Langmiur adsorption isotherm curves for inhibitor molecules

shows the dependence of the degree of the surface covered $\ln(\frac{\theta}{1-\theta})$ as a function of the concentration (ln C_{inh}) of amides. Surface coverage values (θ) for the inhibitor were obtained respectively from potentiodynamic polarization (I_{corr}) measurements for various concentrations at 298 K.

The concentrations of inhibitors, measured as ppm, were calculated as molarity during the plotting of isotherm curves and K_{ads} measurements. The equilibrium constants of the adsorption process were found from the obtained straight lines in $\ln\frac{\theta}{1-\theta} - \ln C$ graphs; which are related to free energy of adsorption Equation 7 where R is the molar gas constant, T is the absolute temperature, and 55.5 is the concentration of water in solution. The equilibrium constant of adsorption process, and K_{ads} and ΔG_{ads} values obtained from Langmuir plot could be seen in Table 3. The values of K_{ads} indicate the strength between adsorbate and adsorbant (metal/organic molecules). The addition of inhibitor causes an increase in the negative values of ΔG_{ads} as can be seen from Table 3. The negative value of ΔG_{ads} shows that the inhibitor is spontaneously adsorbed on the aluminium surface [6, 16, 17]. Values of ΔG_{ads} up to −20kJ/mol are generally consistent with electrostatic interactions between metal and organic molecule (physisorption) while the values around −40 kJ/mol or higher are associated with chemisorptions as a result of sharing them from organic molecules to the metal surface to form a covalent bond [16, 17].

The values of ΔG_{ads} in the measurements ranged from −34.82 to −37.69 kJ/mol in this study. It is suggested that amides (BA, SA, TA) involved both types of interaction; chemisorption and physisorption.

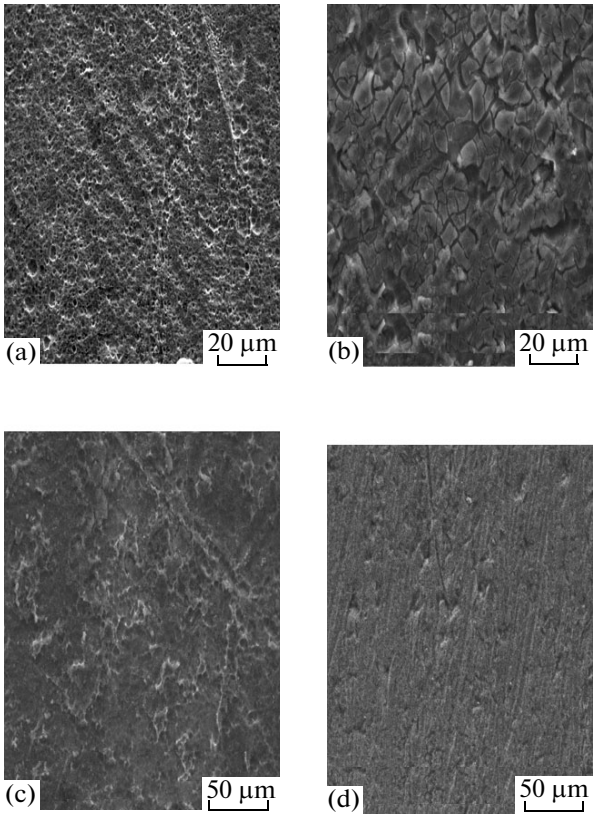

Fig. 10. SEM photographs of aluminium surfaces for five days in (a) 0.1 M NaCl, (b) 100 ppm benzamide, (c) 100 ppm sulfanilamide, d) 100 ppm thioacetamide.

3.4. SEM Analysis

SEM photographs of aluminium plates kept in 0.1M NaCl solutions, with and without inhibitors, for five days can be seen in Figs. 10a–10d. Holes in the metal surface caused by the CI" ions are observed in the NaCl solution without the inhibitors (Fig. 10a). A layer composed of metal oxide and inhibitors on the aluminium surface are observed in the solutions containing 100 ppm benzamide and sulfanilamide (Figs. 10b, 10c). The layer formed in the metal surface of the benzamide solutions was thicker and more porous than in the sulfanilamide solutions. This film layer causes a physical barrier in the metal surface slowing down the corrosion rates of the by limiting the diffusion of ions and molecules from metal surface to solution or from solution to metal surface. No film layer in the metal surface of the thioacetamide solution, as in benzamide and sulfanilamide, was observed in Fig. 10d. This observation showed that thioacetamide formed a complex with the metal atoms. It is thought that this complex did not form an outer layer.

The fact that ΔG_{ad} values were considerably negative strengthened the possibility that metal and thioacetamide molecules formed a complex. In other words,

Table 3. InK, ΔG_{ads} values obtained from Langmiur plot

Inhibitors	ln$K$	$-\Delta G_{ads}$ (kj/mol)
Benzamide	11.2	37.69
Sulfanilamide	10.049	34.82
Thioacetamide	10.89	36.93

a coordinate covalent bond is thought to be formed between metal and organic molecule as a result of the electron transfer from sulfur molecule, the electron charge center, to the metal.

4. CONCLUSIONS

Amides were found to be effective inhibitors for aluminium corrosion in 0.1 M NaCl solutions.

The inhibition efficiency increased with the increase in the concentration. The inhibition efficiencies (IE %) of these compounds followed the sequence TA > SA > BA.

The inhibitor efficiencies determined by EIS and polarization methods are in good agreement.

The corrosion process is inhibited by the adsorption of these molecules on aluminium surface.

The adsorptions of all inhibitors on Al obey the Langmuir's adsorption isotherm rule. The values of both K_{ads} and ΔG_{ads} indicated that all the studied inhibitors are strongly adsorbed on the Al in 0.1 M NaCl.

BA and SA, and TA was determined to be also effective for the prevention of the aluminium corrosion, respectively, by forming a protective layer on the metal surface and by forming a complex with the metal atom, from the SEM photographs.

REFERENCES

1. Sherif, E.M. and Park Su-Moon, *Electrochim. Acta,* 2006, vol. 51, p. 1313.
2. Zor, S.,Yazıcı, B., and Erbil, M., *Corrosion Sci.*, 2005, vol. 47, p. 2700.
3. Zor, S., Dogan, P., and Yazıcı, B., *Corr. Rev.,* 2005, vol. 23, p. 217.
4. Rehim, S.S.A., Hassan, H.H., and Amin, M.A., *Appl. Surf. Sci.*, 2002, vol. 187, p. 279.
5. El-Shafei, A.A., Abd El-Maksoud, S.A., and Fouda, A.S., *Corrosion Sci.*, 2004, vol. 46, p. 579.
6. Obot, I.B. and Obi-Egbedi, N.O., *Collids and Surfaces A: Physicochem. Eng. Aspects*, 2008, vol. 330, p. 207.
7. Lu, H., Li, Y., *Corrosion Sci.*, 2007, vol. 49, p. 4185.
8. Yildirim, A. and Cetin, M., *Corrosion Sci.*, 2008, vol. 50, p. 155.
9. Noor, E.A., *Materials Chemistry and Physics*, 2009, vol. 114, p. 533.
10. Mahmoud, S.S. and El Mohdy, G.A., *Corrosion*, 1997, vol. 53, no. 6, p. 437.
11. Foley, R.T. and Nguyen, T.H., *J. Electrochem. Soc.*, 1982, vol. 129, p. 464.
12. Yazdzad, A.R., Shahrabi, T., and Hosseini, M.G., *Materials Chemistry and Physics,* 2008, vol. 109, p. 199.
13. Badawy, W.A., Al-Kharafi, F.M., and El-Azab, A.A., *Corrosion Sci.,* 1999, vol. 41, p. 709.
14. Sato, N., *Corrosion Sci.*, 1995, vol. 37, p. 1947.
15. Osman, M.M., *Mater. Chem. Phys.,* 2001, vol. 71, p. 12.
16. Yurt, A., *Ulutaş*, S., and Dal, H., *Appl. Surf. Sci.*, 2006, vol. 253, p. 919.
17. Khaled, K.F., Al-Qahtani, M.M., *Materials Chemistry and Physics*, 2009, vol. 113, p. 150.
18. Fang, J. and Li, J., *J. of Molecular Structure (Theochem.),* 2002, vol. 593, p. 179.
19. Ebenso, K., Fekpe, U.J., Ha, B.I., et al., *Materials Chemistry and Physics*, 1999, vol. 60, p. 79.
20. Kandemirli, F. and Sagdinc, S., *Corrosion Sci.*, 2007, vol. 49, p. 2118.
21. Zhang, D.Q., Cai, Q.R., He, X.M., et al, *Materials Chemistry and Physics*, 2008, vol. 112, p.353.
22. Quatarone, G., Battilana, M., Banaldo, L., and Tortato, T., *Corrosion Sci.,* 2008, vol. 50, p. 3467.
23. Hsu, C.H. and Mansfeld, F., *Corrosion*, 2001, vol. 57, p. 747.
24. Goncalves, R.S., Azambujo, D.S., and Serpa Lucho, A.M., *Corrosion,* 2002, vol. 44, p. 467.